Effect of PAMAM Dendrimer Size and pH on the Electrostatic Binding of Metal Complexes Using Cyclic Voltammetry

Agnieszka Kulczynska, Tony Frost, and Lawrence D. Margerum*

Department of Chemistry, University of San Francisco, San Francisco, California 94117

Received June 8, 2006; Revised Manuscript Received July 25, 2006

ABSTRACT: Cyclic voltammetry was employed to investigate the extent of electrostatic binding for metal complexes such as ferrocyanide, $[Fe(CN)_6]^{4-}$, to full generations of polyamidoamine (PAMAM) dendrimers (G1.0−G5.0) as a function of size and pH. Addition of dendrimer solutions to metal complexes caused a large net positive shift in $E_{1/2}$ and reduced peak currents that varied with the size of the dendrimer. Binding ratios, K_{4-}/K_{3-}, calculated from the potential shifts changed from a ratio of five with small dendrimers (G1.0−G3.0) to 10 for G4.0 and G5.0, consistent with known structural changes in PAMAM dendrimers. Conditional binding constants for $[Fe(CN)_6]^{4-}$, calculated from the diffusion-limited oxidation currents, also increased from G3.0 (8.8×10^4 M^{-1}) to G4.0 (31×10^4 M^{-1}). At pH 5, the binding ratios increased dramatically at all generations, suggesting that the interior amine sites in the dendrimer are easily accessible to metal complexes and that dendrimers show some charge selectivity.

Introduction

Dendrimers are a novel class of hyperbranched macromolecules that consist of a polyfunctional core with shells of monomer units extending off of branching points.[1] The resulting macromolecules have well-defined molecular weights and end-group functionality leading to unique applications in such areas as macromolecular catalysis,[2] drug delivery,[3,4] MRI contrast agents,[5,6] and metal ion extraction.[7−9] The appeal of dendrimeric macromolecules is the ability to tailor the structure, shape, and surface functional groups for the application desired.

Perhaps the best-known and studied water-soluble dendrimers are the poly(amidoamine) or PAMAM series of Starburst dendrimers, which are composed of amidoamine monomer units branching out from an ethylenediamine core. Dendrimers are referred to by their generation number, where G*X*.0 is a full generation terminating in primary amines ($X = 0, 1, 2, ...$) and G*X*.5 is a half-generation in which the step-by-step synthesis is terminated in carboxylic acids.[10,11] Potentiometric titrations on the smallest PAMAM, G0.0, gave four closely spaced pK_a's between 9.6 and 8.2 corresponding to the four primary amines and two pK_a's at 6.9 and 3.3 for the core tertiary amines.[12] Other studies using potentiometric titrations and computer simulations on full generations such as G4.0 showed that the terminal primary amines are all protonated by pH 7, while very few of the interior tertiary amines were protonated at this pH. Importantly, negatively charged counterions easily penetrate the PAMAM dendrimers.[13,14] Photochemical and optical absorption differences using charged small molecule probes support a structural change in which the open fluxional lower generations of G2.5 or less transforms to a more rigid spherical structure by G3.5 and beyond.[15−19] Conversely, there is some disagreement as to the effect of solvent and pH on the size and location of terminal groups for the PAMAM series.[20−24] These are important points to resolve as a number of potential applications for dendrimers, including drug delivery and metal ion extraction, require an understanding of small molecule binding as a function of changes in the aqueous environment.

* Corresponding author. E-mail: margeruml@usfca.edu.

The goal of this study is to develop an easy technique for detecting differences in small molecule binding to dendrimers in buffered solutions that may assist researchers in the design of new applications for these unique nanomaterials. The results here draw upon established methods that use voltammetry to measure electrostatic and hydrophobic binding between polyelectroytes, such as DNA and poly(styrenesulfonate), with charged metal complex probes.[25−34] The concentrations of free and bound probe are calculated from the decreases in mass transfer limited currents as the probe binds to the slower diffusing polyelectrolyte during a titration. As opposed to the fixed anionic charge from the sugar−phosphate backbone of DNA, the amine-terminated, full generation PAMAM dendrimers (G*X*.0) accumulate positive charge as a function of decreasing pH. Their surface charge density also changes as a function of generation due to the structural change past G3.5.[35,36] Our hypothesis is that these characteristics should manifest themselves in the binding interactions between PAMAM dendrimers and electrochemically active probes. We present our initial success using cyclic voltammetry to rapidly establish the extent of electrostatic binding of probes, such as ferrocyanide to PAMAM ethylenediamine (ED) core dendrimers as a function of pH and generation.

Experimental Methods

Materials. Methanolic solutions of Starburst polyamidoamine dendrimers with an ED core were purchased from Dendritech Inc. and Aldrich. Dendrimer concentrations are expressed on a molecular basis by using the solution wt % and density from the manufacturer's lot number and the published molar mass. Crystalline potassium ferrocyanide, $K_4[Fe(CN)_6]\cdot 3H_2O$, was obtained from EM Science (Cherry Hill, NJ) and used without further purification. 1,1′-Ferrocenedicarboxylic acid, $[Ru(NH_3)_6]Cl_3$, tris(hydroxymethyl)aminomethane (Tris), and NaCl (99.5%) were purchased and used as received from Sigma-Aldrich.

Procedures. Cyclic voltammetry (CV) was performed inside a Faraday cage with single compartment cells and a model 283 potentiostat controlled by PowerSUITE from Princeton Applied Research (PAR). Glassy carbon (GC) disks (Bioanalytical Systems, BAS) were employed as working electrodes. The GC electrode was polished for each set of experiments with alumina paste (BAS) on a velvet pad followed by ultrasonic cleaning in distilled water and

10.1021/ma061280r CCC: $33.50
Published on Web 09/14/2006

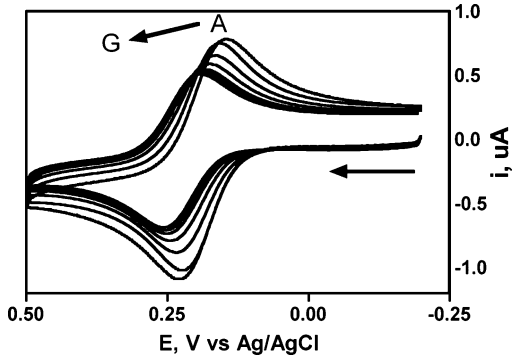

Figure 1. Cyclic voltammograms at a GC electrode for 0.1 mM $[Fe(CN)_6]^{4-}$ in the absence (A) and presence of G2.0 PAMAM (B = 0.011, C = 0.025, D = 0.038, E = 0.052, F = 0.065, G = 0.092 [mM]). Supporting electrolyte is 50 mM NaCl/5 mM Tris, pH 7. Potential scan rate, ν = 50 mV/s.

then rinsing with ethanol. The reference electrode was an Ag/AgCl electrode (BAS) with a Pt wire as the counter electrode. Reported potentials were corrected to either the NHE (normal hydrogen electrode) reference or the Ag/AgCl reference (0.194 V vs NHE). Supporting electrolytes were 50 mM NaCl in 5 mM Tris adjusted to pH 7.0 with HCl or 50 mM NaCl in 5 mM CH_3COONa adjusted to pH 5.0. Solutions of the redox probes were prepared using suitable buffer adjusted to the desired pH. Dendrimer stock solutions were obtained by mixing the commercially available methanolic solutions with purified water in a ratio of 1:9. Concentrated HCl was used to match the probe solution pH.

In a typical titration, 6.0 mL of the redox probe solution was transferred to the cell followed by degassing with buffer saturated argon gas for ~5 min. Argon was directed over the solution to prevent oxygen from reentering the cell during the experiment. The initial current was allowed to attain a constant value (about 10 s) before scanning the potential. For CV, the electrode potential was cycled in an unstirred solution, and the resulting $i-E$ curve was recorded. The curve is described by the Randles−Sevcik equation: $i_{peak} = BCD^{1/2}\nu^{1/2}$, where ν is the scan rate [V/s], $B = Fn^{3/2}A$ (A is electrode area), D is the diffusion coefficient, and C is the concentration of the redox probe.[37] The formal reduction potential ($E^{\circ\prime}$) is taken as the average of the anodic and cathodic peak potentials, $E_{1/2} = (E_{pa} + E_{pc})/2$, for an electrochemically reversible system. Small aliquots of dendrimer stock solution were added to the cell using calibrated digital micropipets, followed by degassing and stirring for at least 5 min. Peak currents and potentials were measured using the peak analysis feature in the software. Prism 4 (GraphPad) was used to fit each data set to the binding isotherm equation using nonlinear regression. The reported binding ratios and binding constants are the mean value of three independent data sets.

Results and Discussion

Typical CV behavior for the sequential addition of G2.0 PAMAM (MW 3256) solution to 0.1 mM $[Fe(CN)_6]^{4-}$ at pH 7.0 are collected in Figure 1. The well-known CV for $[Fe(CN)_6]^{4-}$ in the absence of added dendrimers (curve A) begins at −0.2 V and shows the oxidation of Fe(II) to Fe(III) at a peak potential of 0.214 V vs Ag/AgCl, with a subsequent reduction peak at E_{pc} = 0.150 V after scan reversal. The $E_{1/2}$ is a good approximation of the formal potential and equals 0.182 V (vs Ag/AgCl). The measured value for ΔE_p of 64 mV and the peak current ratio (i_{pa}/i_{pc}) of 1 indicate a reversible one-electron redox process in this buffer composition in accord with literature values.[38] At pH 7 there is general agreement that only the terminal amines on PAMAM dendrimers are charged, so any changes in voltammetry can be attributed to "surface" charge effects.[13] As Figure 1 shows, the redox probe shifts to potentials that are more positive with a corresponding drop in peak current as one adds G2.0.

Scheme 1. Redox Probe Binding to Dendrimers

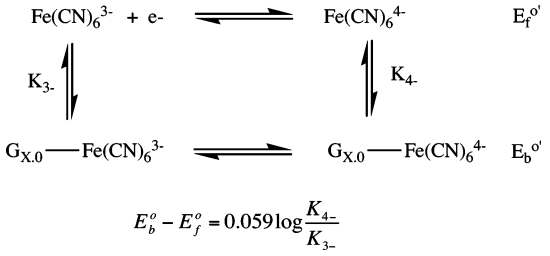

$$E_b^o - E_f^o = 0.059 \log \frac{K_{4-}}{K_{3-}}$$

However, the ΔE_p values and the i_{pa}/i_{pc} ratios are unchanged from curve A. In addition, plots of peak current vs $\nu^{1/2}$ at any given G2.0 concentration remain linear up to 200 mV/s with intercepts of zero (data not shown). These last points establish the measurement as an electrochemically reversible, mass-transfer limited reaction with no electrode absorption effects.

Shifts in Formal Potential with Dendrimer Size. The behavior of $[Fe(CN)_6]^{4-/3-}$ in the presence of G2.0 is reminiscent of the changes in voltammetry seen upon addition of polyelectrolytes to electrophilic redox probes like $[Co(bpy)_3]^{3+/2+}$ at low ionic strength.[26,27,31,32] By analogy, adding dendrimer causes CV peak potentials to shift because of preferential binding of the higher charged form of the probe, while the decrease in peak currents are due to the reduced diffusion coefficient of the probe as it binds to the slower diffusing dendrimer. One may adapt the reaction scheme for probe−DNA work to probe−dendrimer binding in which the difference in formal potential of the fully bound probe ($E_b^{\circ\prime}$) and the free probe ($E_f^{\circ\prime}$) is related to the ratio of binding constants, K_{3-} for ferricyanide and K_{4-} for ferrocyanide, through the Nernst equation (Scheme 1).

Figure 2 shows the shift in $E_{1/2}$ (~$E^{\circ\prime}$) of the probe during titrations of each dendrimer (G2.0−G5.0). The limiting potential shifts are all positive, confirming that the 4− ion binds more strongly than the 3− ion in accord with polyelectrolyte theory. The average $E_{1/2}$ values at the plateau region ($E_b^{\circ\prime}$) lead to the limiting potential shifts and calculated binding ratios (K_{4-}/K_{3-}) shown in Table 1. An interesting trend is apparent in the data. For G1.0 through G3.0, the 4− ion binds 5−6 times more strongly than the 3− ion, but for G4.0 and G5.0 the ratio favoring the 4− ion jumps to 10. This is in direct contrast with cationic probe binding with poly(styrenesulfonate) for which there was no shift in formal potential over a large range of molecular weights.[27] There are several important points to discuss on the basis of these results.

First, despite the 4−/3− charge of the probe, these are surprisingly large equilibrium binding ratios when compared to purely electrostatic probes binding to other polyelectrolytes. For example, Bard's group found that the $[Co(bpy)_3]^{3+/2+}$ binding ratio was 2 with calf thymus DNA using the same buffer

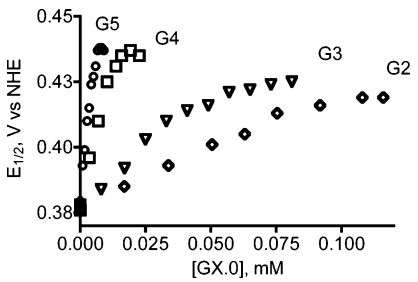

Figure 2. Plots of $E_{1/2}$ determined by CV for 0.1 mM $[Fe(CN)_6]^{4-}$ vs [G*X*.0] in the presence of 50 mM NaCl/5 mM Tris at pH 7. (For clarity, the G1.0 data are not shown.) Each data point is the average of three measurements (standard deviation ca. ±0.002 V).

Table 1. Limiting Potential Shifts and Binding Ratios for $[Fe(CN)_6]^{4-/3-}$ with Dendrimers[a]

PAMAM (ED core)	molar mass	terminal/ interior amines	pH 7		pH 5	
			$E_b - E_f$ (mV)	K_{4-}/K_{3-}	$E_b - E_f$ (mV)	K_{4-}/K_{3-}
G1.0	1430	8/6	44	5.6	ND	ND
G2.0	3256	16/14	45	5.8	85	28
G3.0	6909	32/30	48	6.5	95	41
G4.0	14215	64/62	60	10.2	120	108
G5.0	28825	128/126	61	10.8		*b*

[a] Ratios calculated from equation in Scheme 1. [b] Data not reliable due to periodic electrode fouling.

composition as above, while the Fe(III/II) analogue had a ratio of one (much lower ionic strength began to favor the 3+ ion).[26] Thorp and co-workers found DNA binding ratios favored $[Os(bpy)_3]^{3+}$ over the 2+ ion that ranged from 1.7 at 75 mM NaCl to 3.9 at 15 mM NaCl.[31] One might question the assumption that ferrocyanide acts as a purely electrostatic probe, yet other probes with strong hydrophobic interactions with DNA, like $[M(phen)_3]^{3+/2+}$ complexes, generally gave binding ratios of one or less.[29,31] The electrostatic selectivity we see for even the smallest G*X*.0 PAMAM may have important implications for substrate binding in dendrimer catalytic schemes.

Another implication from the results is that the shift in formal potentials with generation must be due to changes in the physical properties of the macromolecule. The abrupt change in K_{4-}/K_{3-} ratio from a relatively constant value around 5−6 for G1.0−G3.0 to over 10 for G4.0−G5.0 suggests that this redox probe is responding to a size/shape/charge density change and that this change leads to preferential binding of the higher charged ion. Recent studies on PAMAM dendrimers support these observations. For example, transmission electron microscopy (TEM) studies showed that the size and the shape of the PAMAM dendrimers changed abruptly going from lower to higher generations.[39] Computational studies revealed highly asymmetric shapes for G1.0−G3.0, nearly spherical shapes for G5.0−G7.0, and a transitional shape for G4.0. Most recently, Maiti and Goddard extended the computational work to include solvent and pH effects on dendrimer structure. They found a 33% increase in swelling of G5.0 when solvent was included in molecular dynamics simulations. Decreasing the pH increased the radius of gyration and allowed significant water penetration inside the dendrimer.[24] For our results, it is not clear which of these changes may be responsible for the charge selectivity for binding the 4− ion. The pH effects we describe in the next section may be related to both the charge increase and opening of the dendrimer structure as one lowers the pH.

The large binding ratios for G4.0 with $[Fe(CN)_6]^{4-/3-}$ does not extend to a probe with reduced charge, 1,1′-ferrocenedicarboxylic acid. This probe is primarily in the 2− form at pH 7 on the basis of the published pK_a for ferrocenecarboxylic acid of 4.20 in water[40] (the pK_a is 7.76 in 80/20 MeCN/H_2O).[41] The voltammograms of $[Fe(CpCOO^-)_2]^{2-}$ at pH 7 in Figure 3 show that adding G4.0 gives much smaller positive shifts in potentials than earlier. There are also smaller decreases in diffusion currents indicating smaller binding constants, as expected on the basis of the reduced charge of this probe. The K_{2-}/K_{1-} binding ratio calculated from the maximum potential shift is only 1.2 with G4.0. At this point, we cannot rule out a hydrophobic or a hydrogen-bonding interaction between this probe and G4.0 that may decrease the assumed electrostatic binding ratio, although no binding is detectable at pH 9. This result may also point out opportunities and limitations for this technique when selecting probes for these unusual polyelectrolytes.

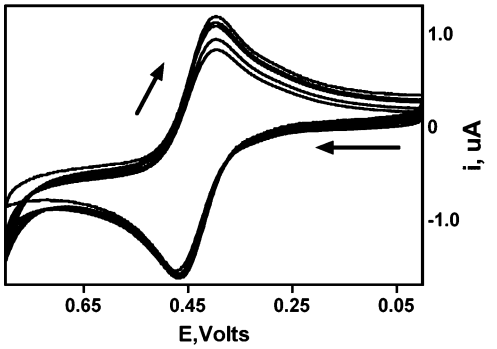

Figure 3. Cyclic voltammograms for 0.29 mM 1,1′-ferrocenedicarboxylic acid showing the effect of added G4.0 dendrimer from 0.003 to 0.040 mM (50 mM NaCl/5 mM Tris at pH 7) at a GC electrode with potential scan rate, $\upsilon = 50$ mV/s.

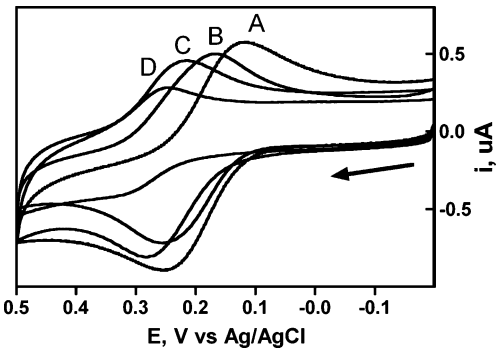

Figure 4. Cyclic voltammograms for 0.1 mM $[Fe(CN)_6]^{4-}$ in the absence (A) and presence of PAMAM dendrimers (B = 0.014 mM G2.0, C = 0.014 mM G3.0, D = 0.013 mM G4.0). Potential scan rate, $\upsilon = 50$ mV/s at a GC electrode in 50 mM NaCl/5 mM acetate buffer at pH 5.

Shifts in Formal Potential with pH. The PAMAM interior tertiary amines are mostly protonated at pH 5, and the shifts in peak potential for the redox probe are much larger than at pH 7 (Table 1). Figure 4 illustrates the magnitude of the potential shifts at pH 5 for $[Fe(CN)_6]^{4-}$ in the absence (curve A) and presence (curves B−D) of about the same concentration G2.0, G3.0, and G4.0 PAMAM dendrimer.

One notices several qualitative changes compared to the pH 7 results. First, potential shifts are much larger at pH 5 than pH 7 for the same concentration of dendrimer. From Figure 4, the shift for G2.0 is +37 mV at pH 5 compared to only +17 mV at pH 7 for the same concentration (data not shown). The shift for G3.0 is +71 mV vs +22 mV, and for G4.0 it is +142 mV compared to +55 mV at pH 7. The larger shifts cause the binding ratios, K_{4-}/K_{3-}, to be much larger at pH 5. Remarkably, the 4− probe appears to bind 100 times more strongly than the 3− probe with G4.0 at pH 5. Second, the electron-transfer reversibility of the free probe and bound probes is not as good in pH 5 acetate buffer ($\Delta E_p = 156$ mV, $i_{pa}/i_{pc} = 0.70$ for free ferrocyanide at scan rate, $\upsilon = 50$ mV/s). Third, as discussed in the next section, the peak current decreases are larger at pH 5 than at pH 7, implying stronger binding constants for the probe at the lower pH, consistent with probe penetration inside the dendrimer. One must keep in mind that the poor electrochemical reversibility makes the binding ratios much less certain at pH 5. In summary, for each PAMAM dendrimer generation, the 4− ion binds much more strongly than the 3− ion at pH 5 than at pH 7, while the structural change in PAMAM dendrimers is still detected since the relative binding ratios jump from 41 to 108 between G3.0 and G4.0.

At this point, one can speculate that the increase in K_{4-}/K_{3-} at lower pH is from the increase in charge density due to

protonation of both the terminal and interior amines. The number of prospective electrostatic binding sites for each generation at pH 5 is almost double compared to pH 7 (see the terminal amine/internal amine ratios in Table 1), so it is not surprising that electrostatic binding should increase. We did not anticipate the large increase in binding ratio with pH, yet the data suggest that the 4− probe must be selectively responding to additional charged sites in the interior of each dendrimer. Another point is that the binding model depicted in Scheme 1 ignores cooperative effects that may shift equilibrium binding to favor the 4− ion or to disfavor 3− binding. While it is not clear which effect may prevail, the dendritic molecule becomes more close-packed and spherelike past G3.0, and the jump in 4−/3− binding ratio could be related to more efficient charge neutralization at the exterior, allowing better access to the interior. In support of this idea, we note that the rheological properties and surface activities of the PAMAM dendrimers in solution depend strongly on the location of the terminal amines.[20−22,24,42]

Finally, titrations at pH 9 with ferrocyanide and G4.0 show no change in peak current or in $E_{1/2}$. Moreover, there is no detectable binding at pH 7 between full generation G*X*.0 dendrimer and the cationic probe, $Ru(NH_3)_6^{3+}$. These are the expected results for purely electrostatic binding, as the PAMAM dendrimers have no charge at high pH and should exclude cations at lower pH.

Voltammetric Peak Current Changes with Dendrimer Generation. As noted above, the peak current for a charged probe decreases as one adds more G*X*.0 dendrimer (pH 7 and below). Voltammetric methods exist to obtain conditional binding constants using the proportionality of current to the diffusion coefficient, *D*, for the free and bound redox probe (for CV the relationship is $i^2 \propto D$). As pointed out by Welch and Thorp, binding constants for redox probes to DNA are obtained by fitting voltammetry currents to the appropriate binding isotherm. They found most electrostatic probes fit best to a binding model that assumed noncooperative or weak territorial binding. Probes such as $Os(bpy)_3^{3+}$ and $Co(bpy)_3^{3+}$, where bpy is 2,2′-bipyridine, gave asymptotic binding isotherms similar to a Scatchard binding model. A biphasic saturation curve (fit to a noncooperative site-binding model) only occurred for strong binding to DNA via intercalation with probes such as $Co(phen)_3^{3+}$ (phen is 1,10-phenathroline) at low ionic strength. The current−concentration relationships from the work reported here are best fits to the weak territorial model. The relationship, derived by Thorp and others for redox probes binding to DNA, is shown in eq 1.[27,31,32]

$$i^2 - i_0^2 = (i_{sat}^2 - i_0^2)\frac{K[\mathrm{G}X.0]}{1 + K[\mathrm{G}X.0]} \qquad (1)$$

where *K* is the conditional binding constant, i_0 is peak current of the free probe, i_{sat} is peak current at binding saturation, and *i* is the peak current during titrations. A measured value for i_{sat} only comes from strong binding probes in the presence of a large excess of dendrimer. Usually, one calculates i_{sat} as a second fitting parameter for weaker binding probes. We find each method yields the same results, so the two-parameter fit is preferred as it saves time and materials. It is important to note that we express the dendrimer concentrations on a molecular basis because the concentration of electrostatic binding sites changes with dendrimer generation and pH (titrations with DNA use the concentration of fixed nucleotide phosphate sites). For a given pH, the titration experiments in this work are conducted under the conditions of $R =$ [electrostatic binding sites]/[probe] > 1, assuming that the number of binding sites is greater than or equal to the terminal amines per dendrimer (Table 1). Figure 5 shows typical $i^2 - i_0^2$ data collected during G2.0−G4.0 titrations of 0.1 mM ferrocyanide at pH 7 along with the two-parameter fit for *K* and i_{sat}. Table 2 contains a summary of the binding constants.

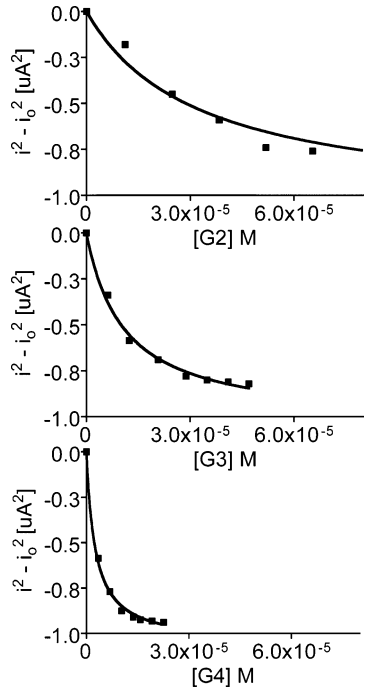

Figure 5. Plots of $i^2 - i_0^2$ during titrations of 0.1 mM $[Fe(CN)_6]^{4-}$ with G*X*.0 in the presence of 5 mM Tris, at pH 7 with 50 mM NaCl added. The solid lines are the nonlinear least-squares fits using eq 1.

Table 2. Conditional Binding Constants at pH 7

generation	K_{4-} (sd) × 10^4 $[M^{-1}]$[a]	generation	K_{4-} (sd) × 10^4 $[M^{-1}]$[a]
G1.0	1.5 ± 0.3	G4.0	31 ± 3
G2.0	2.9 ± 0.2	G5.0	31 ± 7
G3.0	8.8 ± 0.4		

[a] Fit to eq 1 from titration data, for 0.1 mM $[Fe(CN)_6]^{4-}$ in 5 mM Tris/50 mM NaCl.

The calculated binding constant K_{4-} depends on the generation of PAMAM dendrimer, increasing in magnitude from 15 000−88 000 for G1.0−G3.0, but leveling off past 310 000 M^{-1} for both G4.0 and G5.0. This trend tracks the trend in binding ratios seen earlier and reflects stronger binding of the electrostatic probes after the structural change past G3.0. We can only speculate on the leveling off of both the binding ratio and the conditional binding constant K_{4-} at G4.0 and G5.0 as there are numerous variables to consider, such as the effect of pH, surface charge, and counterion binding for each generation. Dubin and co-workers addressed the issue of counterion binding to carboxyl-terminated dendrimers and concluded that effective surface charge density with G5.0 dendrimers may be lower than with G2.0 dendrimers due to strong counterion binding.[43] We see the effect of reduced polyanion charge for a probe molecule through an analysis of the data in Figure 3 for 1,1′-ferrocenedicarboxylic acid. The best fit to the binding isotherm gives $K_{2-} = 2.3 \times 10^4$ M^{-1} with G4.0 at pH 7, a 13-fold decrease compared to the 4− ferrocyanide probe. There are differences in geometry and in the hydrophobic character of ferrocenedicarboxylic acid that may have an effect on binding (i.e., orientation of the carboxylic acid groups toward the dendrimer),

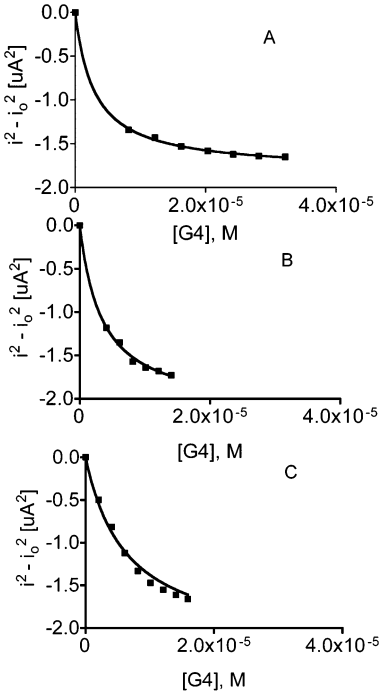

Figure 6. Effect of ionic strength on binding isotherms of 0.1 mM $[Fe(CN)_6]^{4-}$ and G4.0 PAMAM in 5 mM Tris, pH 7 for 15 mM NaCl (A), 75 mM NaCl (B), and 150 mM NaCl (C).

Table 3. Equilibrium Constants for Metal Complexes with Dendrimers at pH 7

probe^n + GX	NaCl, mM	K_n/K_{n-1}	$K_n \times 10^4$, M^{-1}
$[Fe(CN)_6]^{4-}$ + G4.0	150	2.6	15.5
	75	5.1	25.8
	50	10.2	31.1
	15	33.4	44.1
$[Fe(CpCOO^-)_2]^{2-}$ + G4.0	50	1.2	2.3
$[Ru(NH_3)_6]^{3+}$ + G3.5	50	1.0	1.1

but these may be minor effects given the magnitude of the binding constants.

The binding constants calculated in this work compare favorably with other metal complex probes and dendrimers obtained using photochemical data. For example, the binding constant between $[Ru(4,7\text{-}(SO_3C_6H_5)_2\text{-phen})_3]^{4-}$ and G4.0 in pure water was 4.7×10^6 M^{-1}, but decreased with the addition of NaCl.[17] A G4.5 dendrimer (carboxylic acid terminal groups) gave a binding constant of $K = 5.0 \times 10^5$ M^{-1} for $[Ru(phen)_3]^{2+}$ in water, while addition of 0.24 and 0.48 M NaCl decreased the constants to 2300 and 750 M^{-1}, respectively.[18] The excited-state lifetimes of these latter complexes increased with larger PAMAM dendrimers, consistent with a greater charge density on the surface. The binding constant decreased as the salt concentration increased as expected for electrostatic interactions. We also find a decrease in binding constants for redox probes with increasing salt concentrations. Figure 6 shows the voltammetric currents obtained during titration 0.1 mM $[Fe(CN)_6]^{4-}$ with G4.0 in the presence of 15, 75, and 150 mM NaCl. The calculated binding constants are in Table 3. These results are consistent with electrostatic binding as the binding constant increases with decreasing salt concentration and the binding ratio increases to favor the higher charge.

Additional work is underway with other water-soluble dendrimers and a variety of probes to explore possible hydrophobic or hydrogen-bonding effects on binding constants. Preliminary results show that anionic G3.5 PAMAM binds $[Ru(NH_3)_6]^{3+}$ at pH 7 but gives a K_{3+}/K_{2+} binding ratio of one (Table 3).

Conclusions

Electrochemical methods were used in this study to explore electrostatic binding of metal complexes with G1.0−G5.0 PAMAM dendrimers as a function of pH. A simple titration between solutions containing an electroactive probe and dendrimers leads to binding ratios from potential shifts and binding constants from current measurements. The results suggest that the binding ratios obtained from CV potential shifts are an indicator of charge density for the PAMAM dendrimer series. The shell model for the protonation state of the PAMAM series may help explain the phenomena. At pH 7, only the outermost amines (the terminal amines) are charged, and electrostatic binding favors the 4− probe to a small extent. Lowering the pH causes the interior shells (the tertiary amine branching points ending in the ED core) to become charged, and the entire molecule more than doubles it charge by pH 5. While a microscopic explanation of the increased binding ratio (K_{4-}/K_{3-}) at lower pH is not possible from the data, the pH 5 results imply that the macroscopic increase in binding ratio of the 4− probe over the 3− probe is related to an increase in charge density.

The change in electrostatic binding with dendrimer size is perhaps unique for polyelectrolytes. Jiang and Anson saw no changes in the binding of metal complexes to different molecular weights of polystyrenesulfonate (8000−354000) using voltammetry,[27] perhaps due to the random coil nature of these polymers as opposed to the "static" micelle structure of charged dendrimers. Thorp and co-workers found only a small decrease in probe binding to small synthetic nucleic acid polymers compared to DNA and proposed that electrostatic territorial binding is a function of linear charge density as opposed to local charge density.[31]

Clearly, many questions remain on the effect of size, functional group, buffer type, and pH on the binding of small molecules to dendrimers. The CV method, and other electrochemical techniques based on pulse methods, should prove fast and useful for further evaluation of dendrimer polyelectrolyte binding parameters.

Acknowledgment. This work was supported by the University of San Francisco Faculty Development Fund and by a National Science Foundation-Major Research Instrumentation grant for electrochemical equipment (CHE-0216617).

References and Notes

(1) Zimmerman, S. C.; Lawless, L. J. *Top. Curr. Chem.* **2001**, *217*, 95−120.
(2) Kleij, A. W.; Ford, A.; Jastrzebski, J. T. B. H.; van Koten, G. *Dendritic Polymer Applications: Catalysts*; John Wiley & Sons Ltd.: West Sussex, 2001; Chapter III.6.
(3) Lee, C. C.; Yoshida, M.; Frechet, J. M. J.; Dy, E. E.; Szoka, F. C. *Bioconjugate Chem.* **2005**, *16*, 535−541.
(4) Gillies, E. R.; Frechet, J. M. J. *Drug Discovery Today* **2005**, *10*, 35−43.
(5) Stiriba, S.-E.; Frey, H.; Haag, R. *Angew. Chem., Int. Ed.* **2002**, *41*, 1329−1334.
(6) Margerum, L. D.; Campion, B. K.; Koo, M.; Shargill, N.; Lai, J.-J.; Marumoto, A.; Sontum, P. C. *J. Alloys Compd.* **1997**, *249*, 185−190.
(7) Cohen, S. M.; Petoud, S.; Raymond, K. N. *Chem.—Eur. J.* **2001**, *7*, 272−279.
(8) Diallo, M. S.; Balogh, L.; Christie, S.; Swaminathan, P.; Shi, X.; Goddard, W. A., III.; Johnson, J. H., Jr., In *Nanotechnology and the Environment*; Karn, B., Masciangioli, T., Zhang, W., Colvin, V., Alivisatos, P., Eds.; ACS Symposium Series 890; American Chemical Society: Washington, DC, 2005; pp 238−247.
(9) Berndt, U. E. C.; Zhou, T.; Hider, R. C.; Liu, Z. D.; Neubert, H. *J. Mass Spectrom.* **2005**, *40*, 1203−1214.

(10) Tomalia, D. A.; Baker, H.; Dewald, J.; Hall, M.; Kallos, G.; Martin, S.; Roeck, J.; Ryder, J.; Smith, P. *Macromolecules* **1986**, *19*, 2466−2468.
(11) Tomalia, D. A.; Naylor, A. M.; Goddard, W. A., III. *Angew. Chem.* **1990**, *102*, 119−157.
(12) Zhang, Z.; Yu, X.; Fong, L. K.; Margerum, L. D. *Inorg. Chim. Acta* **2001**, *317*, 72−80.
(13) Niu, Y.; Sun, L.; Crooks, R. M. *Macromolecules* **2003**, *36*, 5725−5731.
(14) Cakara, D.; Kleimann, J.; Borkovec, M. *Macromolecules* **2003**, *36*, 4201−4207.
(15) Kleinman, M. H.; Flory, J. H.; Tomalia, D. A.; Turro, N. J. *J. Phys. Chem. B* **2000**, *104*, 11472−11479.
(16) Jockusch, S.; Ramirez, J.; Sanghvi, K.; Nociti, R.; Turro, N. J.; Tomalia, D. A. *Macromolecules* **1999**, *32*, 4419−4423.
(17) Schwarz, P. F.; Turro, N. J.; Tomalia, D. A. *J. Photochem. Photobiol. A* **1998**, *112*, 47−52.
(18) Niu, S.; Turro, C.; Bossmann, S. H.; Tomalia, D. A.; Turro, N. J. *J. Phys. Chem.* **1995**, *99*, 5512−5517.
(19) Turro, N. J.; Barton, J. K.; Tomalia, D. A. *Acc. Chem. Res.* **1991**, *24*, 332−340.
(20) Valachovic, D. E.; Bauer, B. J.; Amis, E. J.; Tomalia, D. A. *Polym. Mater. Sci. Eng.* **1997**, *77*, 230−231.
(21) Topp, A.; Bauer, B. J.; Klimash, J. W.; Spindler, R.; Tomalia, D. A.; Amis, E. J. *Macromolecules* **1999**, *32*, 7226−7231.
(22) Lyulin, A. V.; Davies, G. R.; Adolf, D. B. *Macromolecules* **2000**, *33*, 6899−6900.
(23) Maiti, P. K.; Cagin, T.; Wang, G.; Goddard, W. A., III. *Macromolecules* **2004**, *37*, 6236−6254.
(24) Maiti, P. K.; Cagin, T.; Lin, S.-T.; Goddard, W. A., III. *Macromolecules* **2005**, *38*, 979−991.
(25) Carter, M. T.; Bard, A. J. *J. Am. Chem. Soc.* **1987**, *109*, 7528−7530.
(26) Carter, M. T.; Rodriguez, M.; Bard, A. J. *J. Am. Chem. Soc.* **1989**, *111*, 8901−8911.
(27) Jiang, R.; Anson, F. C. *J. Phys. Chem.* **1991**, *95*, 5701−5706.
(28) Johnston, D. H.; Glasgow, K. C.; Thorp, H. H. *J. Am. Chem. Soc.* **1995**, *117*, 8933−8938.
(29) Welch, T. W.; Corbett, A. H.; Thorp, H. H. *J. Phys. Chem.* **1995**, *99*, 11757−11763.
(30) Johnston, D. H.; Thorp, H. H. *J. Phys. Chem.* **1996**, *100*, 13837−13843.
(31) Welch, T. W.; Thorp, H. H. *J. Phys. Chem.* **1996**, *100*, 13829−13836.
(32) Aslanoglu, M.; Isaac, C. J.; Houlton, A.; Horrocks, B. R. *Analyst* **2000**, *125*, 1791−1798.
(33) Aslanoglu, M.; Oge, N. *Chem. Anal. (Warsaw)* **2004**, *49*, 509−517.
(34) Fan, F.-R. F.; Mazzitelli, C. L.; Brodbelt, J. S.; Bard, A. J. *Anal. Chem.* **2005**, *77*, 4413−4422.
(35) Sun, L.; Crooks, R. M. *J. Phys. Chem. B* **2002**, *106*, 5864−5872.
(36) Chen, W.; Tomalia, D. A.; Thomas, J. L. *Macromolecules* **2000**, *33*, 9169−9172.
(37) Bard, A. J.; Faulkner, L. R. *Electrochemical Methods: Fundamentals and Applications*; Wiley: New York, 1980; p 718.
(38) Sawyer, D. T.; Heineman, W. R.; Beebe, J. M. *Chemistry Experiments for Instrumental Methods;* Wiley: New York, 1984; Chapter 3.
(39) Jockusch, S.; Turro, N. J.; Ottaviani, M. F.; Tomalia, D. A. *J. Colloid Interface Sci.* **2002**, *256*, 223−227.
(40) Pendin, A. A.; Leont'evskaya, P. K.; L'vova, T. I.; Nikol'skii, B. P. *Dokl. Akad. Nauk SSSR* **1969**, *189*, 115−118.
(41) Santis, G.; Fabbrizzi, L.; Licchelli, M.; Pallavicini, P. *Inorg. Chim. Acta* **1994**, *225*, 239−244.
(42) Lee, I.; Athey, B. D.; Wetzel, A. W.; Meixner, W.; Baker, J. R., Jr. *Macromolecules* **2002**, *35*, 4510−4520.
(43) Huang, Q. R.; Dubin, P. L.; Moorefield, C. N.; Newkome, G. R. *J. Phys. Chem. B* **2000**, *104*, 898−904.

MA061280R